



Pharmacokinetic Profile of Gilteritinib: A Novel FLT-3 Tyrosine Kinase Inhibitor

Angela Joubert James¹ · Catherine C. Smith² · Mark Litzow³ · Alexander E. Perl⁴ · Jessica K. Altman⁵ · Dale Shepard⁶ · Takeshi Kadokura⁷ · Kinya Souda⁷ · Melanie Patton¹ · Zheng Lu¹ · Chaofeng Liu¹ · Selina Moy¹ · Mark J. Levis⁸ · Erkut Bahceci¹

Published online: 18 April 2020
© The Author(s) 2020

Abstract

Background and Objective Gilteritinib is a novel, highly selective tyrosine kinase inhibitor approved in the USA, Canada, Europe, Brazil, Korea, and Japan for the treatment of *FLT3* mutation-positive acute myeloid leukemia. This article describes the clinical pharmacokinetic profile of gilteritinib.

Methods The pharmacokinetic profile of gilteritinib was assessed from five clinical studies.

Results Dose-proportional pharmacokinetics was observed following once-daily gilteritinib administration (dose range 20–450 mg). Median maximum concentration was reached 2–6 h following single and repeat dosing of gilteritinib; mean elimination half-life was 113 h. Elimination was primarily via feces. Exposure to gilteritinib was comparable under fasted and fed conditions. Gilteritinib is primarily metabolized via cytochrome P450 (CYP) 3A4; coadministration of gilteritinib with itraconazole (a strong P-glycoprotein inhibitor and CYP3A4 inhibitor) or rifampicin (a strong P-glycoprotein inducer and CYP3A inducer) significantly affected the gilteritinib pharmacokinetic profile. No clinically relevant interactions were observed when gilteritinib was coadministered with midazolam (a CYP3A4 substrate) or cephalexin (a multidrug and toxin extrusion 1 substrate). Unbound gilteritinib exposure was similar between subjects with hepatic impairment and normal hepatic function.

Conclusions Gilteritinib exhibits a dose-proportional pharmacokinetic profile in healthy subjects and in patients with relapsed/refractory acute myeloid leukemia. Gilteritinib exposure is not significantly affected by food. Moderate-to-strong CYP3A inhibitors demonstrated a significant effect on gilteritinib exposure. Coadministration of gilteritinib with CYP3A4 or multidrug and toxin extrusion 1 substrates did not impact substrate concentrations. Unbound gilteritinib was comparable between subjects with hepatic impairment and normal hepatic function; dose adjustment is not warranted for patients with hepatic impairment.

Clinical Trial Registration NCT02014558, NCT02456883, NCT02571816.

1 Introduction

Over 90% of leukemia cases are diagnosed in adults 20 years of age and older, among whom the most common types are chronic lymphocytic leukemia (37%) and acute myeloid leukemia (AML; 32%). [1] It was estimated that 19,520 patients

(10,380 men and 9140 women) would be diagnosed with AML and 10,670 would die of the disease in 2018 in the USA [1].

FLT3, a member of the class III receptor tyrosine kinase family, and its ligand play an important role in the proliferation, survival, and differentiation of multipotent stem cells. FLT3 is over expressed in the majority of AML cases. Activated FLT3 with internal tandem duplications (FLT3-ITD) in and around the juxtamembrane domain, and tyrosine kinase domain mutations at the aspartic acid residue at position 835 (D835), lead to constitutive activation of FLT3. FLT3-ITD and D835 oncogenic mutations occur in approximately 28–34% and 11–14% of patients with AML, respectively, and are associated with a high rate of relapse

Electronic supplementary material The online version of this article (<https://doi.org/10.1007/s40262-020-00888-w>) contains supplementary material, which is available to authorized users.

✉ Angela Joubert James
angela.james@astellas.com

Extended author information available on the last page of the article

Key Points

Dose-proportional pharmacokinetics was observed following once-daily gilteritinib administration (dose range 20–450 mg).

Gilteritinib concentrations peaked at 2–6 h following single and repeat dosing between 20 and 450 mg and exposure when administered 40 mg was comparable under fasted and fed conditions.

Coadministration of gilteritinib with itraconazole (a strong P-glycoprotein inhibitor and cytochrome P450 [CYP] 3A4 inhibitor) or rifampicin (a strong P-glycoprotein inducer and CYP3A inducer) significantly impacted the gilteritinib pharmacokinetic profile; CYP3A4 or multidrug and toxin extrusion 1 substrates did not present clinically relevant drug–drug interactions when coadministered with gilteritinib.

Unbound gilteritinib was comparable between subjects with hepatic impairment and normal hepatic function, thus dose adjustments are not warranted in patients with hepatic impairment.

and a shortened duration of survival [2]. The receptor tyrosine kinase, AXL, also has transformational properties and is involved in the activation of FLT3 [3, 4]. Inhibition of AXL prevents its interaction with FLT3, which in turn blocks the proliferation of *FLT3*-mutant and *FLT3*-wild-type AML cells [3, 4]. In vivo inhibition of AXL was shown to suppress the leukemic burden of *FLT3*-ITD-positive AML in subcutaneous xenograft and leukemia engraftment mouse models [4].

Effective therapies that target FLT3 have been a focus of AML drug development for many years. First-generation FLT3 inhibitors are multi-kinase inhibitors that demonstrate limited efficacy when administered as single agents; second-generation FLT3 inhibitors are more specific and display greater potency than first-generation FLT3 inhibitors. Among the emerging second-generation FLT3 inhibitors, quizartinib, a FLT3/c-Kit/platelet-derived growth factor receptor inhibitor, displayed anti-tumor effects in AML cell lines and antileukemic activity in patients with relapsed/refractory (R/R) AML [5–7]. However, sensitivity to kinase inhibition varied according to the expressed mutant kinase isoform, with *FLT3*-TKD D835V and c-KIT D816 mutant cell lines being far less sensitive to quizartinib [6]. Furthermore, with c-Kit being essential for normal hematopoiesis, simultaneous potent inhibition of FLT3 and c-Kit likely contributed to the myelosuppression observed in patients treated with quizartinib [8, 9].

Gilteritinib (previously known as ASP2215) is a novel, second-generation, small-molecule, oral FLT3 inhibitor recently approved in USA, Canada, Europe, Brazil, Korea, and Japan for the treatment of patients with relapsed or refractory *FLT3* mutation-positive R/R AML. Additionally, in October 2019, the European Commission approved gilteritinib as a single agent for the treatment of patients with *FLT3* mutation-positive R/R AML. Gilteritinib was discovered by Astellas Pharma, Inc. in collaboration with Kotobuki Pharmaceutical Co., Ltd. Preclinical evaluations of gilteritinib showed that it was highly selective for FLT3 with weak activity against c-Kit [10]. Gilteritinib demonstrated highly specific potent inhibition of FLT3 receptors with ITD and D835 mutations and weak activity against FLT3 receptors expressing the F691L gatekeeper mutation [10, 11].

In vivo, gilteritinib inhibited tumor growth and induced tumor regression in mice xenografted with MV4-11 AML cells [10]. A phase I/II dose-escalation/-expansion study (CHRYSALIS study; NCT02014558) evaluated the safety/tolerability, pharmacokinetic (PK), and antileukemic activity of once-daily (QD) gilteritinib as a single agent at doses of 20–450 mg in patients with R/R AML [12]. Gilteritinib was well tolerated with a maximum tolerated dose of 300 mg/day. Potent FLT3 inhibition and dose-proportional PK were observed across all doses [12]. Doses of ≥ 80 mg/day were associated with maximum ($> 90\%$) FLT3 inhibition as well as an overall response rate of 52% and a median overall survival duration of 31 weeks [12].

As clinical evidence regarding gilteritinib therapy continues to accrue, the PK profile, drug interactions, effects of food, and hepatic impairment have been investigated in several phase I clinical studies. Presented here is an overview of the PK profile of gilteritinib in healthy subjects, patients with AML, and other special populations.

2 Methods

2.1 Study Populations

The PK profile of gilteritinib was assessed across five clinical studies (Table 1), including a phase I dose-escalation/-expansion CHRYSALIS study (NCT02014558) in patients with R/R AML ($n = 252$) [12]. In a separate study, gilteritinib absorption, metabolism, and excretion were assessed in patients with advanced solid tumors ($n = 6$). Three studies assessed the clinical PK of gilteritinib in healthy subjects ($n = 121$) and one study assessed the clinical PK of gilteritinib in subjects with impaired hepatic function ($n = 16$). All studies were conducted in accordance with the Declaration of Helsinki and with the approval of the appropriate local ethics committees. Informed consent was obtained from all subjects before study entry.

2.2 Study Designs

2.2.1 CHRYSALIS Study

In this phase I/II study, a total of 252 patients received gilteritinib in one of seven dose cohorts (20–450 mg; $n = 23$, dose escalation; $n = 229$, dose expansion). As a secondary objective, CHRYSALIS characterized single- and multiple-dose PK profiles of gilteritinib in patients with R/R AML as well as assessed potential drug–drug interactions (DDIs) of gilteritinib with concomitant cytochrome P450 (CYP) 3A inhibitors (e.g., voriconazole, posaconazole, and fluconazole) and CYP3A4 and multidrug and toxin extrusion 1 (MATE1) substrates (e.g., midazolam and cephalexin).

For single- and multiple-dose evaluations, full PK profiles for gilteritinib were collected from 23 and 19 patients, respectively. For single-dose evaluation, patients received an initial oral gilteritinib dose followed by a 48-h observation and PK analysis period (Day-2); blood samples were drawn prior to dose (0 h) and at 30 min, and 1, 2, 4, 6, 24, and 48 h post-dose.

Once-daily administration of gilteritinib began following the 48-h observation period used in the single-dose evaluation (Cycle 1 Day 1, 28-day cycles). Multiple-dose PK was investigated on day 15; blood samples were drawn on Cycle 1 Day 15 prior to dose (0 h) and at 30 min, and 1, 4, 6, and 24 h post-dose. In addition, blood samples were collected from all enrolled subjects in the dose-escalation and dose-expansion cohorts prior to dose (0 h) and at 2 h post-dose on Cycle 1 Day 1, Cycle 1 Day 8, on Cycle 1 Day 22, and prior to dose on Day 1 of each cycle starting at Cycle 2. Dose proportionality was assessed using the power model on the area under the concentration–time curve from time of dosing to 24 h post-dose (AUC_{24}) and maximum plasma concentration (C_{max}) after a single dose (Day-2) and after multiple dosing (Day 15). Steady state was determined by visual inspection of gilteritinib median trough concentration (C_{trough}) from Day-2 through Cycle 5 Day 1 (excluding concentration data for patients with dose modifications during this timeframe).

To assess the drug–drug potential of gilteritinib in patients with AML, gilteritinib trough concentration (C_{trough}) data collected for all 252 patients in the CHRYSALIS study were categorized by use of concomitant medications that were CYP3A4 inhibitors: no CYP3A4 inhibitor, moderate CYP3A4 inhibitor, and strong CYP3A4 inhibitor. The potential inhibitory effects of gilteritinib on the PK profile of a CYP3A4 substrate (midazolam) were assessed in a small cohort of 16 patients with R/R AML. Patients received daily doses of gilteritinib 300 mg starting on Cycle 1 Day 1 and a single oral dose of midazolam (2 mg) was administered on Day-1 and Cycle 1 Day 15. Additionally, a small substudy was conducted within the larger CHRYSALIS study to assess the effect of gilteritinib on the PK profile of

cephalexin, a MATE1 substrate. In this cohort, 20 patients received 200-mg daily doses of gilteritinib starting on Cycle 1 Day 1 and a single 500-mg dose of cephalexin administered on Cycle 1 Day-1 and Cycle 1 Day 15.

2.2.2 Mass Balance and Biotransformation Study

In this phase I open-label study, patients ($n = 6$) with advanced solid tumors received QD gilteritinib 120 mg for 2 weeks. On study Day 15, patients received a single-dose of gilteritinib 120 mg (100 μ Ci [14 C]-gilteritinib [1.84 or 1.68 mg/100 μ Ci]) in solution. On study Days 16 through 47, patients again received gilteritinib 120 mg QD. Blood, plasma, urine, and feces samples were collected through Day 47 for absorption, metabolism, and excretion assessments. The metabolic pathway for gilteritinib is postulated based on results from in vitro (liver microsomes and hepatocytes) and in vivo metabolic profiling studies as well as in vitro CYP identification studies using recombinant human CYP-expressing microsomes.

2.2.3 Hepatic Impairment Study

A phase I, open-label, three-arm study was conducted to determine the effects of mild and moderate hepatic impairment on the PK profile of gilteritinib. A total of 24 subjects were enrolled: subjects each with mild ($n = 8$) and moderate ($n = 8$) hepatic impairment, and subjects with normal hepatic function ($n = 8$). The eight healthy subjects with normal hepatic function were approximately matched to subjects with hepatic impairment with respect to age, sex, and body mass index. Hepatic function was categorized using the Child–Pugh classification system with Class A (5–6 points) or Class B (7–9 points) representing mild or moderate severity, respectively.

Each subject received a single oral dose of gilteritinib (10 mg) administered under fasted conditions. Intensive blood sampling was conducted at pre-dose on Day 1 through Day 21 post-dose to assess the plasma pharmacokinetics of gilteritinib. Linear regression was used to analyze the relationship between indices of subjects' hepatic function (baseline serum albumin concentration, prothrombin time, and Child–Pugh score) and gilteritinib PK parameters (area under the concentration–time curve from the time of dosing extrapolated to time infinity [AUC_{inf}] and C_{max}) for the unbound drug. Estimates (slope and intercept) and their corresponding 90% confidence intervals (CIs) are provided for each hepatic function group. An analysis of covariance with hepatic impairment group as a factor and sex as covariate was performed. The parameters of interest were the log-transformed AUC_{inf} , area under the concentration–time curve from the time of dosing to 480 h post-dose, and C_{max} . The least-squares mean (LSM) of the primary parameters for

Table 1 Gilteritinib clinical pharmacokinetic (PK) studies

Study	Populations	Previously published PK results	Key eligibility	Dose
Dose escalation/expansion (CHRYSA-LIS) Phase I/II NCT02014558	Overall population: 252 male and female patients with R/R AML, ~70% of whom were receiving concomitant strong (voriconazole or posaconazole) or moderate (fluconazole) CYP3A4 inhibitors CYP3A4 substrate (midazolam) subpopulation: 16 patients with R/R AML MATE1 substudy: 20 patients with R/R AML	Yes [12, 22]	Aged ≥ 18 years with R/R AML with <i>FLT3</i> mutation (ITD and/or activating point mutation)	Dose escalation: gilteritinib 20, 40, 80, 120, 200, 300, and 450 mg administered QD CYP3A4 substrate (midazolam): midazolam (2 mg of syrup) was administered as a single oral dose on study Days -1 and Day 15 of Cycle 1; gilteritinib (300 mg) was administered QD starting on Day 1 of Cycle 1 MATE1 substudy: gilteritinib was administered with cephalixin (500-mg oral tablet or capsule) as a single oral dose on Day-1 and Day 15 of Cycle 1
Mass balance and biotransformation Phase I NCT02456883	Six male and female patients with solid tumors	No	Aged ≥ 18 years with a confirmed diagnosis of advanced solid tumor for which no standard therapy was available	Gilteritinib 120 mg QD on Days 1–14 and 16–47; [¹⁴ C]gilteritinib 120 mg (100 µCi) single dose under fasted conditions on Day 15
Hepatic impairment Phase I NCT02571816	24 male and female subjects: eight subjects with mild hepatic impairment, eight with moderate hepatic impairment, and eight healthy subjects with normal hepatic function	No	Aged 18–75 years, BMI range of 18.5–34.0 kg/m ² , criteria for mild-to-moderate hepatic impairment were based on the Child–Pugh classification	Single dose of gilteritinib 10 mg under fasted conditions
CYP3A4 drug–drug interaction Phase I	81 healthy male and female subjects: 21 patients in Cohort 1 and 20 patients in Cohorts 2–4, each	No	Aged 18–55 years, BMI range of 18.5–34.0 kg/m ² , and weighed ≥ 50 kg at screening	Cohort 1: Single-dose gilteritinib 10 mg (Day 1) Cohort 2: 200-mg ITCZ BID on Day 1 and 200 mg QD on Days 2–28, with single-dose gilteritinib 10 mg administered on Day 6 Cohort 3: 400-mg FLCZ on Day 1 and 200 mg QD on Days 2–28, with single-dose gilteritinib 10 mg administered on Day 6 Cohort 4: 600-mg RIF QD on Days 1–21, with gilteritinib 20 mg administered on Day 8
Effect of food Phase I	32 healthy male and female subjects: 16 per cohort	No	Aged 18–55 years, BMI range of 18.5–34.0 kg/m ² , and weighed ≥ 50 kg at screening	Single dose of gilteritinib 40 mg under fasted or fed (high-fat breakfast) conditions

AML acute myeloid leukemia, BID twice daily, BMI body mass index, CYP cytochrome P450, FLCZ fluconazole, ITCZ itraconazole, ITD internal tandem duplication, MATE multidrug and toxin extrusion, QD once daily, R/R relapsed/refractory, RIF rifampicin

each impairment group was estimated and the 90% CI was constructed around the difference between the LSM of each impairment group and the normal hepatic function group. Both the difference between the LSM and the 90% CIs were back transformed to the original scale and expressed as percentages.

2.2.4 Cytochrome P450 3A4 Drug–Drug Interaction Study

In a phase I DDI study, 81 healthy subjects were randomly assigned 1:1:1:1 to one of four cohorts: Cohort 1: gilteritinib 10 mg alone on Day 1 ($n=21$); Cohort 2: gilteritinib 10 mg (Day 6) plus itraconazole (a strong CYP3A4 and P-glycoprotein [P-gp] inhibitor) administered 200 mg twice daily (Day 1) and 200 mg QD (Days 2–28) [$n=20$]; Cohort 3: gilteritinib 10 mg (Day 6) plus fluconazole (a moderate CYP3A4 inhibitor) administered 400 mg (Day 1) and 200 mg twice daily (Days 2–28) [$n=20$]; Cohort 4: gilteritinib 20 mg (Day 8) plus rifampicin (a strong CYP3A4 inducer) 600 mg (Days 1–21) [$n=20$]. Plasma samples were collected for up to 24 days after dosing with gilteritinib in Cohort 1, 29 days after gilteritinib dosing in Cohorts 2 and 3, and 22 days after gilteritinib dosing in Cohort 4. In Cohorts 2 and 3, plasma samples were also collected prior to the daily dose of itraconazole or fluconazole, respectively, on Days 7, 10, 13, 15, and 22, and 24 h post-dose on Day 29. In Cohort 4, plasma samples were collected prior to the daily dose of rifampicin on Days 8, 10, 13, and 15, and 24 h post-dose on Day 22.

To assess the DDI potential of gilteritinib, 90% CIs estimated for the geometric LSM (GLSM) ratios were used: itraconazole (combination/gilteritinib alone), fluconazole (combination/gilteritinib alone), and rifampicin (combination/gilteritinib alone) to assess each drug's effect on the PK profile of gilteritinib, or midazolam (combination/midazolam alone) and cephalexin (combination/cephalexin alone) to assess the effect of gilteritinib on their PK profiles. To assess the DDI potential of gilteritinib, a mixed-effects model was fitted on natural logarithm-transformed C_{\max} , area under the concentration–time curve from the time of dosing to the last measurable concentration (AUC_{last}), and AUC_{inf} , with treatment as the fixed effect and subject as a random effect; for each PK parameter, a 90% CI was constructed for the GLSM ratio of gilteritinib plus itraconazole, fluconazole, or rifampicin (test) to gilteritinib alone (reference).

2.2.5 Effect of Food Study

A phase I, open-label, randomized, single-dose, parallel-design, food-effect study was performed in healthy subjects. A total of 32 subjects were randomized (1:1) to receive 40 mg of gilteritinib following an overnight fast of at least 10 h or were administered the standard US Food and Drug Administration high-fat, high-calorie breakfast. Blood

samples were collected pre-dose (0 h) and post-dose through Day 23; intensive sampling was conducted on Day 1. To assess the effect of food on the PK profile of gilteritinib, an analysis of variance model with fixed effects for treatment (fed or fasted) was fitted on natural logarithm-transformed C_{\max} , AUC_{last} , area under the concentration–time curve from the time of dosing to 72 h post-dose (AUC_{72}), and AUC_{inf} . Within the analysis of variance, the LSM differences between fed and fasted, along with 90% CI on the differences, were estimated. The LSM for C_{\max} , AUC_{last} , AUC_{72} , and AUC_{inf} were back transformed to produce the GLSM and presented with the number of subjects for each treatment. The GLSM ratio and its corresponding 90% CIs for each PK parameter are presented by back transforming and are expressed as percentages.

2.3 Bioanalytical Methods

Plasma samples were collected for PK evaluations and analyzed with validated bioanalytical methods based on high-performance liquid chromatography with tandem mass spectrometry using an internal standard. The calibration range of the analytical method for both plasma and urine is 0.1–50 ng/mL or 10–5000 ng/mL, and 0.5–250 ng/mL, respectively.

Itraconazole and its major metabolite, 2-hydroxyitraconazole, as well as fluconazole and rifampicin plasma concentrations, were assayed using validated high-performance liquid chromatography with tandem mass spectrometry methods. The calibration range was 0.500–500 ng/mL for itraconazole and 2-hydroxyconazole, 20–10,000 ng/mL for fluconazole, and 100–10,000 ng/mL for rifampicin. Quality control samples to evaluate the accuracy and precision of a ten-fold dilution for itraconazole and a two-fold dilution for fluconazole were also included in the assay development. No quality control dilution samples were used for rifampicin. The predominant circulating plasma metabolites (AS3397391 [M17], AS3322943 [M16], and AS2651096 [M10]) were quantitated using a validated liquid chromatography with a tandem mass spectrometry assay method with a lower limit of quantification of 0.5 ng/mL, respectively.

2.4 Pharmacokinetic Analysis

Pharmacokinetic parameters were estimated by noncompartmental analyses using Phoenix WinNonlin (version 6.3 or higher). The estimated PK parameters included C_{\max} , time to C_{\max} (T_{\max}), pre-dose plasma concentration, area under the concentration–time curve from time zero to infinity, terminal half-life ($t_{1/2}$), apparent clearance, and apparent volume of distribution. Apparent clearance and apparent volume of distribution were calculated using a population PK analysis; results of this analysis will be reported in a manuscript

that is currently under development. Dose proportionality was assessed by the power model involving regression of the logarithmically transformed area under the concentration–time curve from time zero to infinity vs dose.

3 Results

3.1 Study Participants

Demographics and baseline characteristics of healthy subjects and patients with advanced solid tumors or R/R AML are detailed in Table 2.

3.2 Dose-Escalation/Dose-Expansion Study (CHRYSALIS)

Gilteritinib exhibited dose-proportional pharmacokinetics in patients with R/R AML at doses from 20 to 450 mg administered QD (Fig. 1, Fig. 1 and Table 1 of the Electronic Supplementary Material [ESM]). Following oral administration of gilteritinib, peak gilteritinib concentrations (C_{max}) were observed between 2 and 6 h following single and repeat dosing; $t_{1/2}$ and T_{max} did not appear to be dose dependent. Steady state appears to be achieved by Day 15 based on gilteritinib C_{trough} (Fig. 2). At 120 mg, the recommended phase II dose, the median C_{max} and AUC_{24} were 282 ng/mL and 6180 ng·h/mL, respectively, after multiple-dose administration. The estimated $t_{1/2}$ was from 45 to 159 h and up to ten-fold accumulation based on the accumulation index (Table 3).

At doses of ≥ 80 mg, gilteritinib steady-state C_{trough} was associated with greater therapeutic effect. Composite complete response, defined as the sum of patients achieving complete response, complete response with incomplete hematological recovery, or complete response with incomplete platelet recovery occurred more commonly in patients with gilteritinib steady-state $C_{trough} \geq 100$ ng/mL (Fig. 3), which can be achieved at QD gilteritinib doses of 80 mg or greater.

The effects of CYP3A4 inhibitors were also assessed in patients with R/R AML in the CHRYSALIS study. Dose-normalized gilteritinib C_{trough} from patients are summarized in Fig. 2. Although the data indicate a trend of increasing gilteritinib exposure when gilteritinib was administered with a moderate or strong CYP3A4 inhibitor relative to patients who do not use a CYP3A4 inhibitor, the observed increase is less than two-fold. This magnitude of increased exposure is not considered clinically significant and suggests gilteritinib is moderately sensitive to CYP3A4 inhibition.

Within the CHRYSALIS study, the potential inhibitory effects of gilteritinib on the PK of a CYP3A4 substrate (midazolam) was assessed in a small cohort of 16 patients with R/R AML. Gilteritinib was administered QD starting

Table 2 Demographic and baseline characteristics

Sex	Dose escalation/expansion (n = 252)	Mass balance and biotransformation (n = 6)	Hepatic impairment			CYP3A4 drug–drug interaction			Food effects		
			Mild (n = 8)	Moderate (n = 8)	Normal (n = 8)	GIL (n = 21)	ITCZ + GIL (n = 20)	FLCZ + GIL (n = 20)	RIF + GIL (n = 20)	Fed (n = 16)	Fasted (n = 16)
Male	129 (51)	3 (50)	5 (63)	5 (63)	5 (63)	19 (91)	20 (100)	19 (95)	18 (90)	14 (88)	14 (88)
Female	123 (49)	3 (50)	3 (37)	3 (37)	3 (37)	2 (9)	0	1 (5)	2 (10)	2 (12)	2 (12)
Race											
White	213 (85)	6 (100)	7 (88)	8 (100)	8 (100)	12 (57)	9 (45)	13 (65)	12 (60)	6 (38)	9 (56)
Other	39 (15)	0	1 (12)	0	0	9 (43)	11 (55)	7 (35)	8 (40)	10 (62)	7 (44)
Age, years ^a	62 (21–90)	59 (49–75)	58.5 (55–65)	53.5 (48–65)	54 (48–58)	33 (22–53)	32 (22–55)	40.5 (20–54)	31.5 (22–49)	39 (26–54)	38 (29–51)
Weight, kg ^b	75.3 (18.1)	88.2 (34.0)	73.9 (14.6)	76.5 (15.1)	74.4 (17.5)	80.2 (12.2)	80.7 (11.0)	79.6 (10.5)	76.4 (9.5)	78.1 (8.7)	81.6 (11.6)
BMI, kg/m ^{2b}	26.1 (5.6)	32.8 (9.7)	27.0 (5.6)	28.0 (4.5)	27.2 (4.2)	25.97 (3.02)	25.6 (2.6)	25.7 (2.8)	25.2 (1.9)	25.9 (2.5)	26.5 (2.8)

AME absorption, metabolism, and excretion, BMI body mass index, CYP cytochrome P450, DDI drug–drug interaction, FLCZ fluconazole, GIL gilteritinib, ITCZ itraconazole, RIF rifampicin

Data presented as n (%) unless otherwise indicated

^aData presented as median (range)

^bData presented as mean (standard deviation)

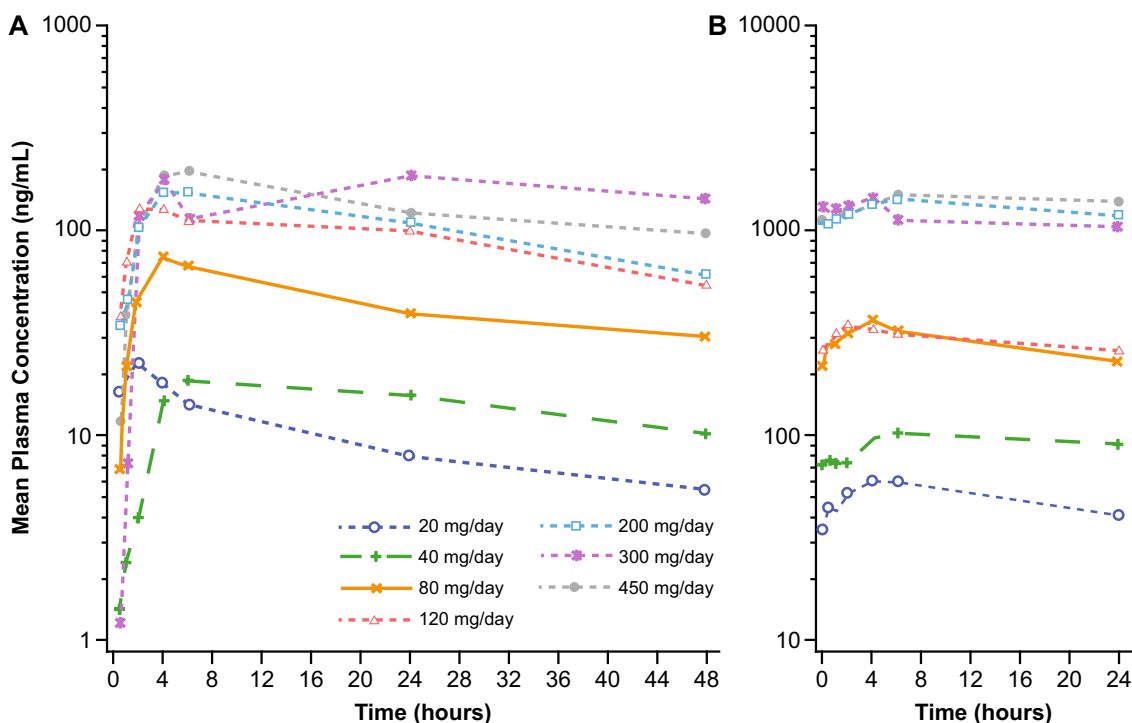


Fig. 1 Mean plasma gilteritinib concentrations after escalating oral doses in patients with acute myeloid leukemia (AML). Single-dose concentration–time curve (a) and multiple-dose concentration–time

curve (b). Single dose (Cycle 1 Day-2), 20 mg: *n*=5; 40–450 mg: *n*=3. Steady state (Cycle 1 Day 15), 20 mg: *n*=4; 40 mg, 80 mg, 120 mg, 300 mg: *n*=3; 200 mg: *n*=2; 450 mg: *n*=1

on Day 1 of Cycle 1. Relative to administration of midazolam alone, coadministration of gilteritinib with midazolam resulted in a 10% increase (not significant) in midazolam C_{max} and AUC_{24} (Fig. 4, Table 4). Both C_{max} and AUC_{24} of the major midazolam metabolite, 1-hydroxymidazolam,

were also increased by approximately 23% and 50%, respectively.

In a substudy of 20 patients, coadministration of gilteritinib with cephalexin did not result in markedly different cephalexin exposure or urinary excretion compared to that

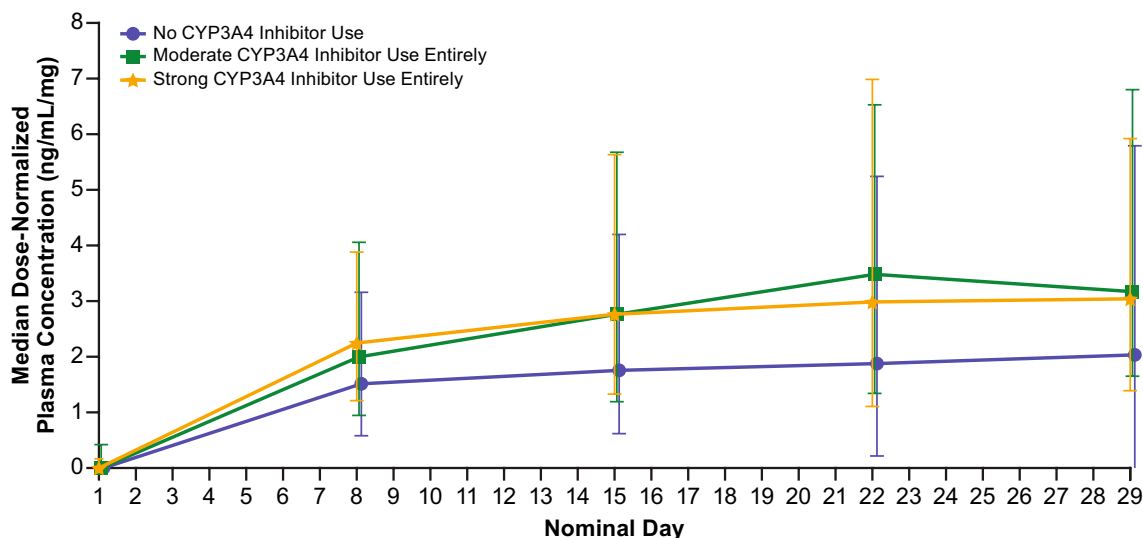


Fig. 2 Median dose-normalized gilteritinib trough plasma concentration–time profiles by use of a cytochrome P450 (CYP) 3A inhibitor in patients with relapsed or refractory acute myeloid leukemia (AML)

Table 3 Gilteritinib pharmacokinetic parameters after single (Day-2) and multiple administrations (Day 15), CHRYSALIS

Single dose							
Parameter	20 mg (n=5)	40 mg (n=3)	80 mg (n=3)	120 mg (n=3)	200 mg (n=3)	300 mg (n=3)	450 mg (n=3) ^a
<i>C</i> _{max} (ng/mL)							
Mean (SD)	28.1 (21.5)	25.0 (14.6)	75.3 (25.2)	137 (94.4)	168 (45.3)	204 (136)	208 (51.8)
Median (range)	23.7 (7.5–64.5)	16.99 (16.3–41.8)	71.5 (52.2–102)	85.7 (78.9–246)	149 (136–220)	137 (115–361)	216 (152–255)
AUC ₂₄ (ng·h/mL)							
Mean (SD)	302 (207)	360 (223.5)	1216 (473)	2480 (1972)	3022 (844)	4163 (3178)	3324 (221.1)
Median (range)	262 (98.5–642)	315 (163–603)	995 (895–1759)	1393 (1291–4756)	2538 (2533–3997)	2446 (2214–7830)	3324 (3168–3480)
<i>T</i> _{max} (h)							
Median (range)	2.0 (0.50–4.0)	5.98 (3.97–24.0)	4.0 (4.0–4.1)	2.1 (2.0–3.8)	5.2 (4.0–5.97)	6.1 (4.1–24.1)	5.8 (4.1–5.92)
Multiple dosing							
Parameter	20 mg (n=4) ^b	40 mg (n=3) ^c	80 mg (n=3)	120 mg (n=3)	200 mg (n=2)	300 mg (n=3)	450 mg (n=1)
<i>C</i> _{max} (ng/mL)							
Mean (SD)	64.6 (48.8)	108 (31.92)	376 (150.5)	374 (190)	1462 (815)	1525 (665)	1528
Median (range)	45.6 (30.5–137)	106 (76.7–140)	396.3 (217–516)	282 (248–593)	1462 (886–2038)	1257 (1036–2282)	
AUC ₂₄ (ng·h/mL)							
Mean (SD)	1299 (1006)	2482 (33.3)	6958 (3273)	6943 (3221)	31,428 (21,412)	31,005 (10,068)	34,768
Median (range)	917.0 (540–2440)	2482 (2458–2505)	6234 (4108–10,532)	6180 (4171–10,477)	31,428 (16,288–46,568)	28,711 (22,282–42,022)	
<i>T</i> _{max} (h)							
Median (range)	4.0 (4.0–6.0)	3.9 (0.50–6.0)	4.3 (4.0–4.4)	2.2 (1.95–5.75)	6.0 (6.0–6.1)	6.1 (4.1–6.1)	5.93
<i>t</i> _{1/2} (h)							
Mean (SD)	62.1 (17.9)	152 (129.2)	86.1 (24.1)	45.9 (18.83)	142 (61.5)	142 (55.0)	NC
Median (range)	54.46 (49.4–82.6)	151.8 (60.5–243)	91.03 (60.0–107)	44.93 (27.5–65.1)	142 (98.4–185)	159 (80.7–187)	
<i>R</i> _{ac}							
Mean (SD)	4.3 (1.069)	9.6 (7.8)	5.7 (1.4)	3.3 (1.2)	9.0 (3.7)	9.1 (3.3)	NC
Median (range)	3.8 (3.5–5.5)	9.6 (4.2–15.1)	6.0 (4.1–6.97)	3.2 (2.2–4.4)	9.0 (6.4–11.7)	10.1 (5.4–11.7)	
<i>C</i> _{trough} (ng/mL)							
Mean (SD)	n=11 43.5 (23.5)	n=12 72.9 (40.1)	n=20 165 (88.0)	n=61 367 (253)	n=79 816 (557)	n=15 1242 (723)	n=1 1170
Median (range)	43.4 (13.6–37.5)	66.6 (26.7–166)	110 (78.6–339)	292 (77.1–1173)	668 (90.5–2925)	1085 (470–2391)	

AUC₂₄ area under the concentration–time curve from time of dosing to 24 h post-dose, *C*_{max} maximum plasma concentration, *C*_{trough} trough concentration, NC not calculated, *R*_{ac} accumulation ratio, *SD* standard deviation, *t*_{1/2} elimination ratio (calculated from *R*_{ac}), *T*_{max} time to reach maximum concentration

^an=2 for AUC₂₄

^bn=3 for AUC₂₄, *t*_{1/2}, and *R*_{ac}

^cn=2 for AUC₂₄, *t*_{1/2}, and *R*_{ac}

observed after administration of cephalexin alone, as evidenced by GLSM ratios: 91.5% for *C*_{max}, 94.0% for AUC_{inf}, 97.7% for AUC_{last}, and 82.8% for renal clearance (Fig. 5, Table 5). These findings suggest that coadministration of gilteritinib with a MATE1 substrate is not expected to result in a clinically relevant DDI.

3.3 Mass Balance and Biotransformation Study

Of the six enrolled patients, four patients were evaluable for mass balance and characterization of gilteritinib and [¹⁴C]-radioactivity PK and five patients were evaluable for metabolite profiling. One patient was non-evaluable for mass

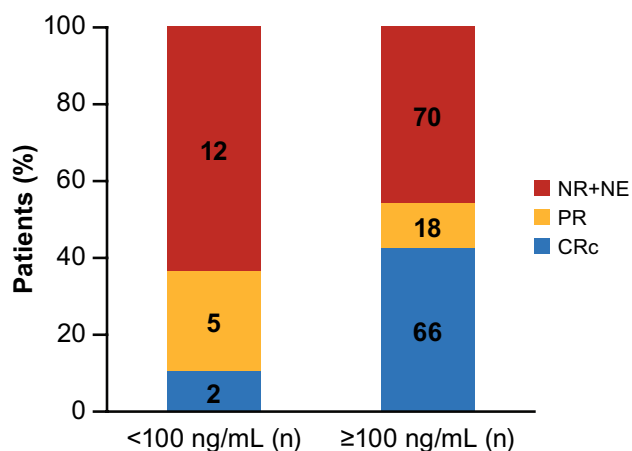


Fig. 3 Relationship between gilteritinib trough concentration and clinical response. Numbers inside the bars represent the number (*n*) of patients achieving each response, while the proportion (%) of patients achieving each response is represented on the y axis. All patients who received at least one dose of the study drug for whom sufficient plasma concentration data were available to facilitate the derivation of at least one pharmacokinetic (PK) parameter, and for whom the time of dosing on the day of sampling was known, were included in the analysis. *CRc* composite complete response, *n* number of patients, *NE* not evaluable, *NR* no response, *PR* partial response

balance because of difficulty voiding, resulting in low recovery of the administered dose. Another patient was administered a dose of non-radiolabeled gilteritinib prior to collection of the 24-h sample on Day 16. For this patient, plasma and whole blood concentration data at 24 h post-dose were excluded from the descriptive statistics of plasma and blood concentration data and summary PK parameters.

In vivo plasma protein binding in humans is approximately 94%, and gilteritinib is primarily bound to albumin (data on file). Average total blood-to-plasma ratios of total ¹⁴C-radioactivity had a range of 0.8514–1.361, indicating low partitioning of gilteritinib into blood. These results parallel data from rodent and canine PK studies (data on file, Astellas Pharma, Inc.).

Based on in vitro metabolism data, gilteritinib is primarily metabolized via CYP3A4. Quantified metabolites in humans include M17 (formed via *N*-dealkylation and oxidation), M16, and M10 (both formed via *N*-dealkylation); these metabolites were also observed in animals (data on file). None of the three metabolites exceeded 10% of the overall parent exposure. The proposed metabolic schemes for gilteritinib in humans are provided in Fig. 6.

Data demonstrated gilteritinib is primarily excreted in feces. After a single oral dose of ¹⁴C-gilteritinib, 64.5% of the total administered dose was recovered in feces. Renal excretion is a minor elimination pathway, with 16.4% of the total dose recovered in urine. Gilteritinib plasma concentrations declined in a bi-exponential manner with an estimated

half-life of 113 h based on a population PK analysis (not shown).

In this study, oral bioavailability of gilteritinib is estimated to be greater than 61.2%, based on the sum of excretion percentages of the parent gilteritinib in urine and metabolites in urine (16.4%) and feces (64.5%), and 80.9% of the total radioactive dose recovered (Fig. 2 and Table 2 of the ESM). Unchanged gilteritinib (parent) was the most abundant radioactive peak, accounting for 6.3–15.8% and 11.7–23.8% in urine and feces, respectively.

The peak corresponding to M10 accounting for 0.4–2.1% and 6.3–10.3% in urine and feces, respectively, also included other minor metabolites. The postulated metabolic pathways involve at least: (1) oxidation of methylpiperazine (M6, M8, and M14), piperidine (M17), oxane (M9, M12, and M15), and an unspecified moiety (M1); (2) *N*-dealkylation of methylpiperazine (M2, M7, and M10) and piperidine (M16 and M17); (3) glutathione conjugation (M3, M5, M11, and M13); and (4) glucuronidation (M4). The metabolite-to-parent ratios of the three predominant circulating metabolites identified in plasma (AS3397391 [M17], formed via oxidation, AS3322943 [M16], and AS2651096 [M10], both formed via *N*-dealkylation) were each less than 10% of the parent overall exposure.

3.4 Hepatic Impairment Study

A decrease in gilteritinib exposure (AUC_{inf} and C_{max}) was observed with increasing severity of hepatic impairment. Although differences in total C_{max} and area under the concentration–time curve (AUC) were observed in subjects with hepatic impairment compared with healthy subjects with normal hepatic function, these differences were not apparent when gilteritinib exposure parameters were corrected for protein binding, indicating that unbound gilteritinib exposure in subjects with mild or moderate hepatic impairment is comparable to that observed in subjects with normal hepatic function (Table 6). As such, mild (Child–Pugh Class A) or moderate (Child–Pugh Class B) hepatic impairment does not have a clinically meaningful effect on the PK profile of gilteritinib; the effect of severe hepatic impairment (Child–Pugh Class C) on the PK of gilteritinib was not evaluated.

3.5 Cytochrome P450 3A4 Drug–Drug Interaction Study

The effect of strong and moderate CYP3A4 inhibitors and a strong CYP3A4 inducer on the PK of gilteritinib was evaluated in an open-label parallel-group study in 81 healthy subjects. Coadministration of itraconazole resulted in a significant increase (~2.2-fold) in the systemic exposure of gilteritinib (Fig. 7). A smaller increase in gilteritinib

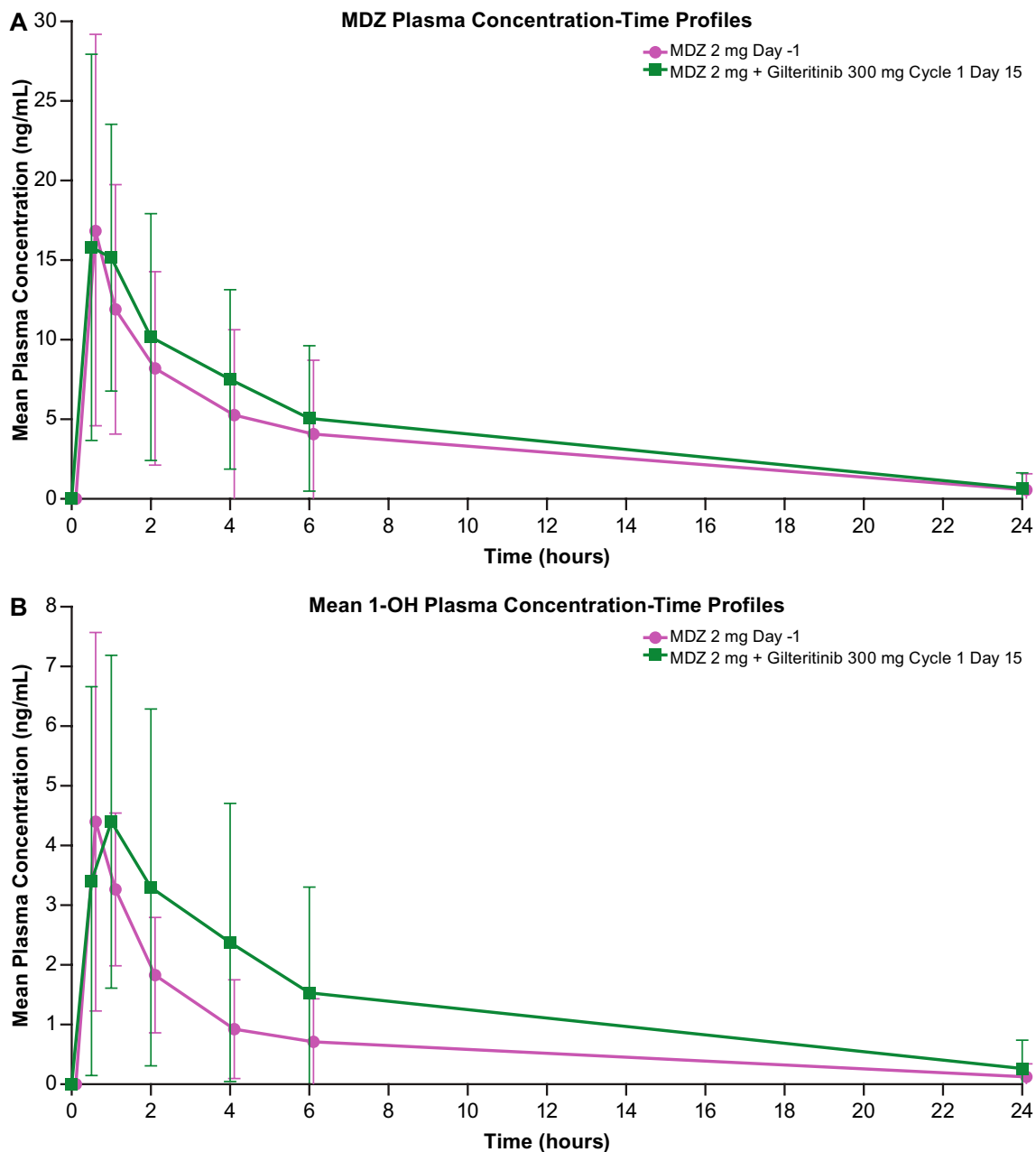


Fig. 4 Mean midazolam [MDZ] (a) and 1-OH midazolam (b) plasma concentration–time profiles in patients with relapsed or refractory acute myeloid leukemia (AML). Concentrations below the limit of quantification (BLQ) [lower limit of quantification (LLOQ)=0.1 ng/

mL] were set to zero. Mean was not calculated if concentration was BLQ for all subjects in a given category. Day-1, $n=15$ at 24 h; Cycle 1, Day 15, $n=8$ at 24 h. 1-OH 1-hydroxymidazolam

systemic exposure (~1.43-fold) was observed following coadministration of gilteritinib with fluconazole. Concomitant administration of rifampicin significantly decreased gilteritinib systemic exposure by ~70%.

Pre-dose plasma concentrations of itraconazole and fluconazole were maintained at exposures demonstrated to inhibit CYP3A4 [13]. Pre-dose concentrations of rifampicin

were less than the lower limit of quantification in Table 7, all subjects, at all timepoints (Days 8, 10, 13, 15, and 22). As a result, it was not possible to confirm rifampicin exposure during the treatment period.

Taken together, coadministration of gilteritinib with a strong CYP3A4 inhibitor or inducer may result in significantly greater or lesser, respectively, gilteritinib systemic

Table 4 Effect of gilteritinib on the pharmacokinetics of midazolam, CHRYSALIS

Comparison	Analyte	N	Parameter	MDZ + gilteritinib (GLSM)	MDZ alone (GLSM)	GLSM ratio ^a (%)	90% CI
Midazolam + gilteritinib/ midazolam alone	MDZ	8	AUC ₂₄ (ng•h/mL)	59.4	54.3	109.5	49.8–240.5
	MDZ	9	C _{max} (ng/mL)	16.0	14.3	111.6	69.5–179.3
	1-OH MDZ	8	AUC ₂₄ (ng•h/mL)	17.0	11.3	149.9	74.9–300.1
	1-OH MDZ	9	C _{max} (ng/mL)	4.3	3.5	123.5	72.4–210.5

1-OH MDZ 1-hydroxymidazolam, AUC₂₄ area under the concentration–time curve from time of dosing to 24 h post-dose, CI confidence interval, C_{max} maximum observed concentration, GLSM geometric least-squares mean, MDZ midazolam

^aValue of 100 indicates no change

exposure. As itraconazole is also a P-gp inhibitor, observed increased gilteritinib exposure may be due to inhibition of P-gp.

3.6 Effect of Food Study

In 32 healthy subjects, the rate and extent of gilteritinib absorption were slightly decreased, although not statistically significant, when coadministered with a high-fat meal, as evidenced by GLSM ratios: 74.0% for C_{max}, 91.0% for AUC₇₂, 93.8% for AUC_{inf}, and 94.6% for AUC_{last} (Table 8).

4 Discussion

This report provides a comprehensive characterization of the clinical PK of gilteritinib, a highly selective tyrosine kinase inhibitor (TKI) used in the treatment of cancer, and the effect of intrinsic and extrinsic patient factors. Gilteritinib exhibits linear dose-proportional PK in patients with R/R AML at doses with a range of 20–450 mg. Gilteritinib undergoes rapid absorption, with a median T_{max} observed between 2 and 6 h following single and multiple dosing, and was eliminated slowly with an estimated t_{1/2} range of 45–159 h; t_{1/2} and T_{max} do not appear to be dose dependent. Furthermore, administration of gilteritinib with a high-fat breakfast did not affect the overall exposure (AUC_{inf}, AUC_{last}, and AUC₇₂) of gilteritinib, suggesting that gilteritinib can be administered without any food-related considerations.

In the CHRYSALIS study, data indicated a trend of increasing gilteritinib exposure when gilteritinib was administered with a moderate or strong CYP3A4 inhibitor relative to patients who did not use a CYP3A4 inhibitor; the observed increase was less than two-fold. This magnitude of increased exposure is not considered clinically significant. A review of drug-related safety events categorized by CYP3A4 inhibitor use did not indicate differences in the incidence of safety events in patients coadministered a moderate or strong CYP3A4 inhibitor compared with patients not administered a CYP3A4 inhibitor. Changes in gilteritinib exposure that

are less than two-fold (or 200%) are not considered clinically relevant based on (a) the European Medicines Agency and Food and Drug Administration definition of a sensitive substrate (i.e., plasma AUC increased two-fold or more) and (b) whether the magnitude of increased exposure leads to serious adverse events [14]. As gilteritinib is not a drug with a narrow therapeutic index [14], moderate increases in exposure are not expected to result in a significant increase of adverse events, as evidenced by the comparable incidence of drug-related safety events in patients with R/R AML who were coadministered strong CYP3A inhibitors and gilteritinib relative to patients who did not receive strong CYP3A inhibitors during gilteritinib therapy.

That said, the 2.2-fold increase observed in gilteritinib exposure when coadministered with a strong CYP3A4 inhibitor supports precautionary use of strong CYP3A4 inhibitors during gilteritinib therapy. Clinicians are advised to use alternative therapies that are not strong CYP3A inhibitors if possible. Caution is also advised when administering gilteritinib, a P-gp substrate, with strong P-gp inhibitors, most of which are also strong CYP3A inhibitors. Coadministration of gilteritinib and combined P-gp and strong CYP3A inducers is prohibited because of the significant reduction in gilteritinib exposure. Coadministration of gilteritinib with midazolam or cephalexin did not result in markedly different midazolam or cephalexin exposures; therefore, coadministration of CYP3A4 and MATE1 substrates with gilteritinib is not restricted. Additionally, a loss of efficacy in subjects with low or moderate hepatic impairment (based on the Child–Pugh definition) is not anticipated, as unbound gilteritinib exposure in subjects with hepatic impairment was comparable to that in subjects with normal hepatic function. Therefore, gilteritinib dose adjustment is not warranted for patients with low or moderate hepatic impairment. The clinical PK studies discussed above support use of a single daily dose, where virtually all patients achieve an effective drug concentration. Furthermore, gilteritinib can be taken with or without food and, in patients with AML, may be used in combination with some commonly used CYP3A inhibitors, e.g., azole antifungals.

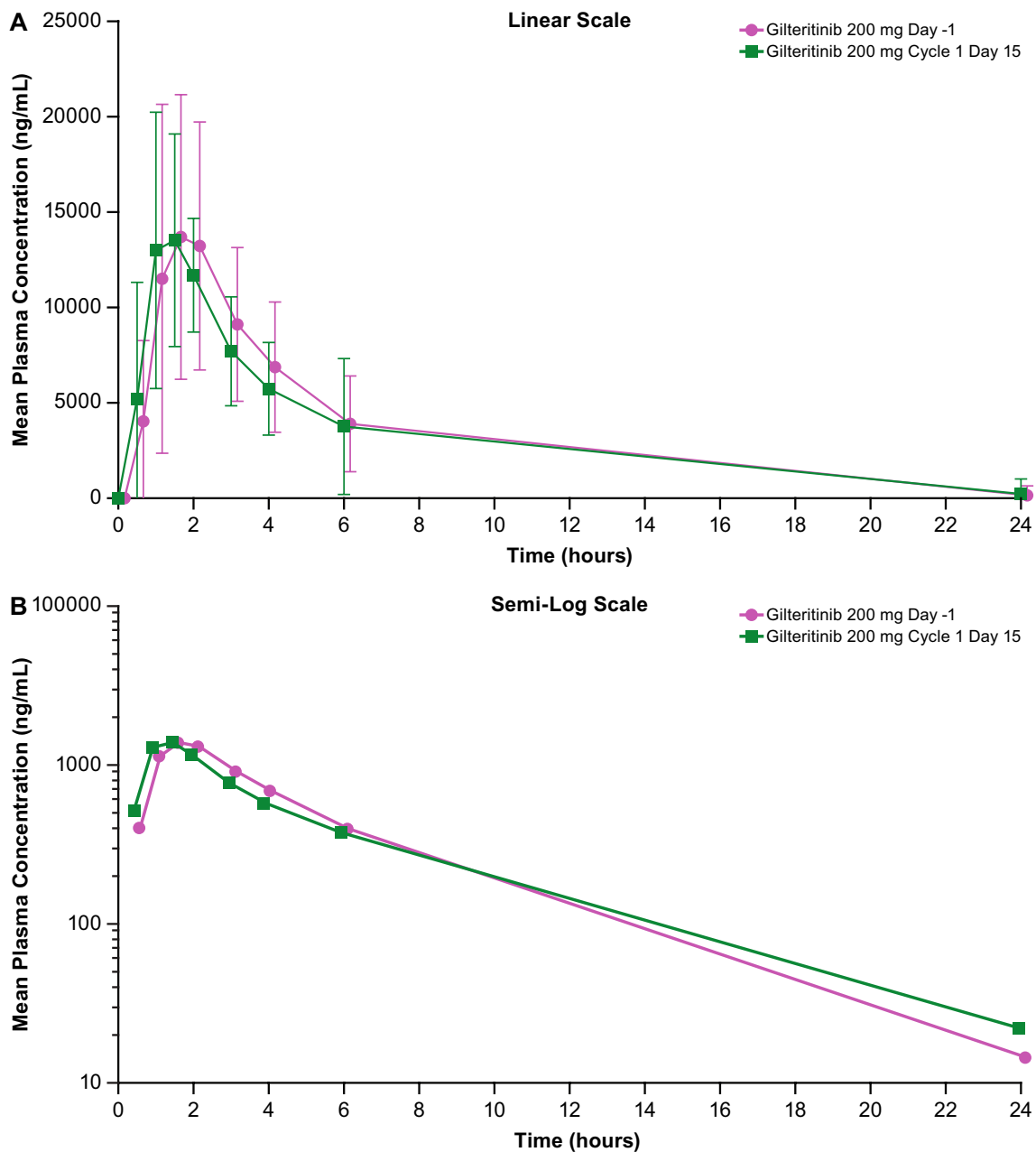


Fig. 5 Effect of gilteritinib on the pharmacokinetics of cephalexin in patients with relapsed or refractory acute myeloid leukemia (AML). Linear scale (a) and Log scale (b). Day-1, $n=20$ at 24 h; Cycle 1, Day 15, $n=16$ at 24 h

Regarding the dose-proportional PK of gilteritinib in the CHRYSALIS study, range and median T_{max} were generally the same across doses, especially at steady state (Cycle 1 Day 15). More variability was observed after single-dose administration but given the small sample size of the dose cohorts ($n=3-5$ patients) and a patient population with various comorbidities and concomitant medications, high inter-subject variability is not unexpected. Still, the median T_{max} was generally consistent in patients with R/R AML and healthy subjects. To better characterize the sources of

variability in PK, a population analysis (results not shown) demonstrated that although some covariates reflecting intrinsic and extrinsic traits were statistically significant such that their inclusion in the model improved data fitting, their impact on gilteritinib exposure was not clinically significant.

Since the approval of the first TKI, imatinib, in 2011, at least 23 TKIs have been approved in the USA [15] and 14 in Europe [16], including midostaurin (RYDAPT), approved for the treatment of adults with newly diagnosed *FLT3* mutation-positive AML, in combination with standard cytarabine

Table 5 Effects of gilteritinib on cephalixin pharmacokinetics after administration of cephalixin alone or coadministered with gilteritinib, CHRYSALIS (substudy)

PK parameter	<i>N</i>	Cephalixin alone GLSM	Cephalixin and gilteritinib GLSM	GMR (%) ^a	90% CI ^a
AUC_{inf} (ng•h/mL)	12	54,066	50,802	93.96	(75.29–117.26)
AUC_{last} (ng•h/mL)	16	50,808	49,647	97.71	(74.19–128.70)
C_{max} (ng/mL)	16	16,946	15,498	91.46	(74.60–112.12)
Ae (mg)	10	436.9	366.7	83.93	(46.53–151.39)
CLr (L/h)	6	10.67	8.842	82.84	(40.25–170.48)

Ae cumulative amount of unchanged drug excreted into the urine, AUC_{inf} area under the concentration–time curve from the time of dosing extrapolated to time infinity, AUC_{last} area under the concentration–time curve from the time of dosing to the last measurable concentration, CI confidence interval, CLr renal clearance, C_{max} maximum observed concentration, $GLSM$ geometric least-squares mean, PK pharmacokinetic

^aThe difference of a least-squares mean of log-transformed PK parameters between cephalixin alone and cephalixin and gilteritinib and its 90% CI are back transformed to the raw scale and values are expressed as percentages

and daunorubicin induction and cytarabine consolidation. The PK of these TKIs have been well characterized in the literature [17, 18]. Similar to many of the approved TKIs, gilteritinib has moderate oral bioavailability (estimated to be greater than 61.2%), is rapidly absorbed (median T_{max} between 2 and 6 h), moderately bound to plasma proteins (94%), primarily albumin, and is a CYP3A substrate. A few distinguishing attributes of the PK of gilteritinib are its long half-life (113 h), lack of food effect, and lack of clinically significant drug interaction with strong and moderate CYP3A inhibitors. In contrast, midostaurin has a shorter half-life (21 h), its exposure increases by 1.6-fold with a high-fat meal, and it has a 10.4-fold and 2.1-fold increase in exposure when coadministered with ketoconazole or itraconazole, respectively.

Gilteritinib has a large volume of distribution. These results parallel data from rat and dog PK studies (data not shown). In vivo plasma protein binding in humans is approximately 90% and gilteritinib is primarily bound to albumin. Average total blood-to-plasma ratios of [¹⁴C]-radioactivity as measured in the human mass balance and biotransformation study had a range of 0.8514–1.361, indicating a low association of gilteritinib with blood cellular components.

The PK characteristics of gilteritinib are quite similar to those observed for other approved TKIs, all of which are CYP3A4 substrates. Moreover, population PK (results not shown, manuscript in development) was performed on data pooled across patient and healthy subject studies. When using the subject type as the covariate, the population-estimated half-life in patients with R/R AML (not shown) is 113 h and is comparable to that observed in healthy subjects.

One limitation of the analysis of the effect of CYP3A inhibitors on the PK of gilteritinib in patients with R/R AML is that the characteristic exposure parameters, i.e., C_{max} and AUC, could not be determined for gilteritinib because of insufficient data in the planned DDI cohort in the phase I

study in patients with R/R AML. Instead, a post hoc exploratory analysis comparing C_{trough} in patients who were receiving a strong or moderate CYP3A inhibitor was performed on the data. Although it is not the standard approach, the current analysis is based on steady-state concentration data as opposed to a single-dose study and is more reflective of the real-world concomitant use of strong CYP3A inhibitors, many of which are azole antifungals used to treat infection in this patient population. It is also important to note the relative timing of administration of CYP3A inhibitors to gilteritinib administration was not considered in the current analysis.

Another limitation regarding assessment of drug interactions with CYP3A inhibitors and inducers is that the probes used, itraconazole, fluconazole, and rifampicin, are also P-gp inhibitors (itraconazole, fluconazole) or inducers (rifampicin). Hence, the contribution of CYP3A or P-gp inhibition or induction, respectively, on the observed effect cannot be discerned. However, this does allow for the estimation of the maximum change in gilteritinib exposure due to dual inhibitory or induction effects. As such, the product labeling for gilteritinib includes restrictions related to concomitant use of “combined P-gp and strong CYP3A inducers” and cautionary use of strong CYP3A/P-gp inhibitors while being treated with gilteritinib. This language reflects the large overlap of drugs that have dual inhibitor or inductive effects on CYP3A and P-gp.

In the drug–drug interaction with rifampicin, there were no measurable concentrations of rifampicin because of its short half-life (3.5 h) [19] relative to the QD sampling schema. At least 7 days of rifampicin administration (600 mg) is required for maximal enzyme induction prior to dosing the “victim” drug [20]. To maintain enzyme induction, especially for drugs with long half-lives, rifampicin should continue to be administered for at least 11–14 days. Although we were not able to measure rifampicin

Fig. 6 Proposed metabolic pathway for gilteritinib

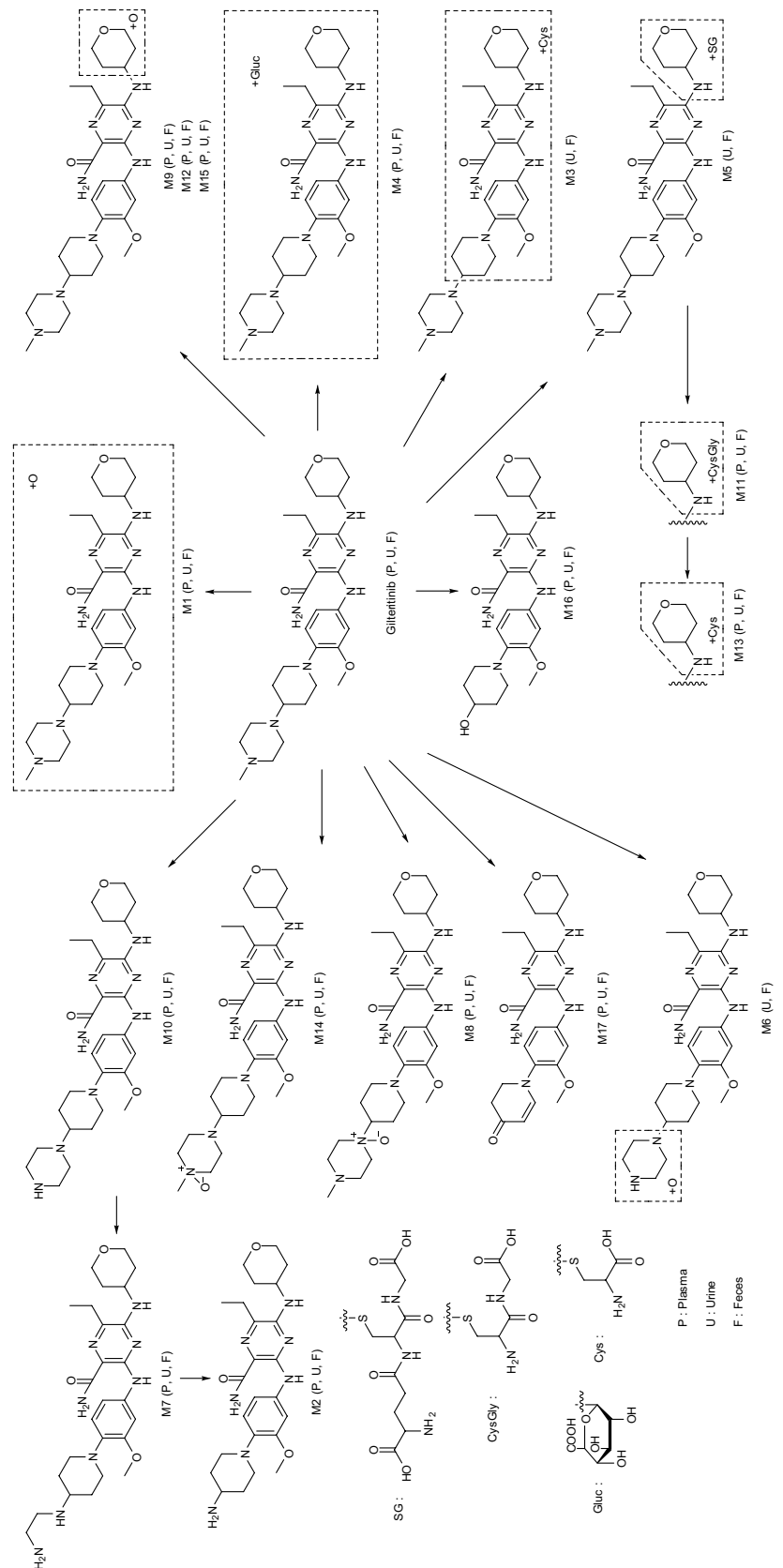


Table 6 Statistical analysis of hepatic impairment on total and unbound gilteritinib pharmacokinetics

Parameter	Hepatic function	N	GLSM ^a		GMR (%) ^b		90% CI ^b	
			Total	Unbound	Total	Unbound	Total	Unbound
AUC _{inf} (h•ng/mL)	Mild	8	433.3	27.53	78.88	88.42	(61.1–101.8)	(65.9–118.6)
	Moderate	8	337.4	27.54	61.43	88.48	(47.6–79.3)	(66.0–118.7)
	Normal	8	549.3	31.13	NA	NA	NA	NA
AUC ₄₈₀ (h•ng/mL)	Mild	8	408.4	25.95	78.13	87.59	(60.8–100.4)	(65.9–116.4)
	Moderate	8	316.5	25.84	60.55	87.21	(47.1–77.8)	(65.6–115.9)
	Normal	8	522.7	29.62	NA	NA	NA	NA
C _{max} (ng/mL)	Mild	8	8.140	0.5171	106.59	119.49	(82.1–138.4)	(91.3–156.5)
	Moderate	8	6.242	0.5095	81.73	117.72	(63.0–106.1)	(89.9–154.2)
	Normal	8	7.637	0.4328	NA	NA	NA	NA

AUC₄₈₀ area under the concentration–time curve from the time of dosing to 480 h post-dose, AUC_{inf} area under the concentration–time curve from the time of dosing extrapolated to time infinity, CI confidence interval, C_{max} maximum observed concentration, GLSM geometric least-squares mean, GMR geometric mean ratio, NA not applicable

^aThe exponentiated value of the least-squares mean based on natural log-transformed data

^bAssessment based on an analysis of variance with a fixed effect for hepatic function group was performed on natural log-transformed parameters. Ratios and confidence limits are transformed back to raw units by exponentiating and values are expressed as percentages. The ratio denotes the hepatic function group GLSM estimate divided by the normal hepatic function group GLSM estimate

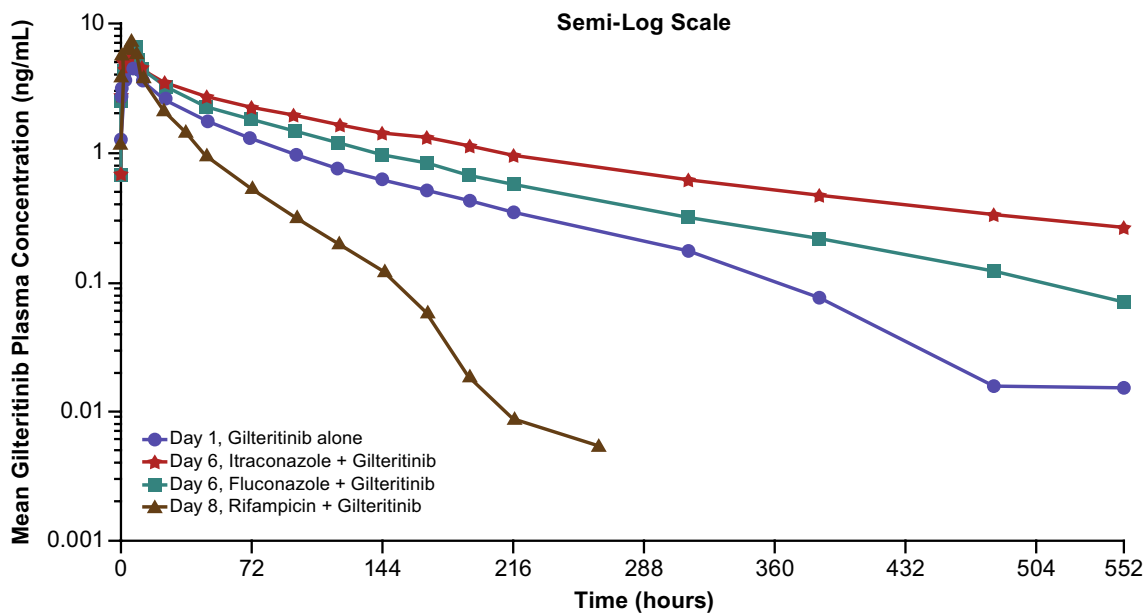


Fig. 7 Effects of strong cytochrome P450 (CYP) 3A4 inhibitors and inducers on mean gilteritinib plasma concentrations in healthy adult subjects. Concentrations below the limit of quantification (BLQ)

[lower limit of quantification (LLOQ)=0.1 ng/mL] were set to zero. Mean was not calculated if concentration was BLQ for all subjects in a given category. N=20 for each treatment arm

concentrations, the dosing period of rifampicin (21 days) prior to (7 days) and after (14 days) gilteritinib drug administration is similar to that noted in the literature, which has established the timeframe and rifampicin exposure needed for adequate and sustained induction of CYP3A [21].

There were also some challenges regarding the mass balance study, which are typically conducted in healthy

subjects. As gilteritinib has marked accumulation after multiple-dose administration (reflecting its intended use), the study was designed so that absorption, metabolism, and elimination could be evaluated at steady state. Hence, the study was conducted in patients with solid tumors given the potential genotoxicity of gilteritinib. Given the long half-life, the sample collection period spanned 28 days. As in-patient

Table 7 Effect of strong cytochrome P450 3A4 inhibitors and inducers on the pharmacokinetic profile of gilteritinib in healthy adult subjects

Treatment	Parameter	Gilteritinib + inducer/ inhibitor (GLSM)	Gilteritinib alone (GLSM)	GLSM ratio ^a (%)	90% CI
Itraconazole + gilteritinib/gilteritinib alone	AUC _{inf} (ng•h/mL)	67.7	30.6	221.4	188.3–260.4
	AUC _{last} (ng•h/mL)	61.5	28.8	213.5	180.6–252.4
	C _{max} (ng/mL)	0.593	0.495	119.8	100.1–143.4
Fluconazole + gilteritinib/gilteritinib alone	AUC _{inf} (ng•h/mL)	43.9	30.6	143.5	122.0–168.7
	AUC _{last} (ng•h/mL)	41.5	28.8	144.0	121.8–170.3
	C _{max} (ng/mL)	0.573	0.495	115.7	96.7–138.5
Rifampicin + gilteritinib/gilteritinib alone	AUC _{inf} (ng•h/mL)	8.71	30.6	28.5	24.2–33.5
	AUC _{last} (ng•h/mL)	8.42	28.8	29.2	24.7–34.5
	C _{max} (ng/mL)	0.364	0.495	73.4	61.4–87.9

AUC_{inf} area under the concentration–time curve from the time of dosing extrapolated to time infinity, AUC_{last} area under the concentration–time curve from the time of dosing to the last measurable concentration, CI confidence interval, C_{max} maximum observed concentration, GLSM geometric least-squares mean

^aValue of 100 indicates no change

Table 8 Effects of food on the pharmacokinetic (PK) profile of gilteritinib

PK parameter	N	Fed GLSM	Fasted GLSM	GMR (%) ^a	90% CI ^a
AUC _{inf} (ng•h/mL)	16	1900	1780	93.8	81.2–108.4
AUC _{last} (ng•h/mL)	16	1840	1740	94.6	81.8–109.3
AUC ₇₂ (ng•h/mL)	16	951	865	91.0	78.2–105.9
C _{max} (ng/mL)	16	28.6	21.2	74.0	62.2–88.1

AUC₇₂ area under the concentration–time curve from the time of dosing to 72 h post-dose, AUC_{inf} area under the concentration–time curve from the time of dosing extrapolated to time infinity, AUC_{last} area under the concentration–time curve from the time of dosing to the last measurable concentration, CI confidence interval, C_{max} maximum observed concentration, GLSM geometric least-squares mean, GMR geometric mean ratio

^aAssessment based on an analysis of variance performed on natural log-transformed parameters with the food condition as a fixed effect. Ratios and confidence limits are transformed back to a raw scale and values are expressed as percentages. The ratio denotes the gilteritinib 40-mg fed GLSM estimate divided by the gilteritinib 40-mg fasted GLSM mean estimate

confinement was not feasible for this duration, intermittent outpatient periods were integrated into the study. However, samples were not collected during the outpatient periods, therefore limiting greater recovery of the total administered dose.

5 Conclusions

In summary, gilteritinib exhibits a clinical PK profile that supports QD administration with or without hepatic impairment. Gilteritinib has been approved as a single agent for R/R AML with *FLT3* mutations. The clinical PK studies discussed above support use of a single daily dose, where

virtually all patients achieve an effective drug concentration. Furthermore, gilteritinib can be taken without regard to food and may be taken concomitantly with strong CYP3A inhibitors, many of which are antifungal agents commonly used to treat infection in patients with R/R AML.

Acknowledgments We acknowledge all patients and subjects for their participation, as well as the investigators, coordinators, and site personnel involved in these studies. Named authors meet the International Committee of Medical Journal Editors criteria for authorship for this manuscript, take responsibility for the integrity of the work as a whole, and have given final approval to the version to be published. All authors had full access to all of the data in this study and take complete responsibility for the integrity of the data and accuracy of the data analysis. Writing and editorial assistance under the authors' guidance was provided by Regina Switzer, PhD, and Patrick Tucker, PhD, of OPEN Health Communications, LLP (Chicago, IL, USA) and was funded by Astellas Pharma, Inc.

Funding This research was sponsored by Astellas Pharma, Inc. (Northbrook, IL, USA).

Compliance with Ethical Standards

Conflict of Interest Angela Joubert James, Melanie Patton, Chaofeng Liu, Selina Moy, and Erkut Bahceci are employees of Astellas Pharma, US Inc. Zheng Lu was an employee of Astellas Pharma US, Inc. during the time of the study and development of the manuscript. Takeshi Kadokura and Kinya Souda are employees of Astellas Pharma, Inc. Catherine C. Smith received research grants from Astellas Pharma US, Inc. Mark Litzow has no conflicts of interest that are directly relevant to the content of this article. Alexander E. Perl has received funding, honoraria, or travel reimbursement from Astellas, Daiichi-Sankyo, Arog, Novartis, Pfizer, Actinium Pharmaceuticals, Jazz Pharmaceuticals, Takeda, AbbVie, NewLink Genetics, Asana Biosciences, and Seattle Genetics. Jessica K. Altman has received funding, honoraria, or travel reimbursement from AbbVie, Agios, Ariad, Astellas, Bayer, BioSight, BMS, Boehringer Ingelheim, Cancer Expert Now, Celator, Celgene, Daiichi Sankyo, Epizyme, France Foundation, FujiFilm, Genentech, Glycomimetics, GSK, Incyte, Janssen Pharmaceuticals, Novartis, PeerView, Pfizer, prIME Oncology, Syros, and Theradex.

Dale Shepard has received funding, honoraria, or travel reimbursement from Celgene, Sanofi, AstraZeneca, Ipsen, Amgen, Genentech, Eli Lilly, Bayer, Leap, Alkermes, Aduro, Halozyme, Ignyta, BMS, Pfizer, Kinex, and Corvus. Mark J. Levis has received funding or personal fees from Astellas, Novartis, Daiichi-Sankyo, and FujiFilm.

Consent to Participate For investigations involving human subjects, informed consent was obtained from the participants involved.

Data Sharing Researchers may request access to anonymized participant-level data, trial-level data, and protocols from Astellas-sponsored clinical trials at www.clinicalstudydatarequest.com. For the Astellas criteria on data sharing, see <https://clinicalstudydatarequest.com/Study-Sponsors/Study-Sponsors-Astellas.aspx>.

Ethics Approval The research was conducted within all the appropriate ethical and legal guidelines.

Open Access This article is licensed under a Creative Commons Attribution-NonCommercial 4.0 International License, which permits any non-commercial use, sharing, adaptation, distribution and reproduction in any medium or format, as long as you give appropriate credit to the original author(s) and the source, provide a link to the Creative Commons licence, and indicate if changes were made. The images or other third party material in this article are included in the article's Creative Commons licence, unless indicated otherwise in a credit line to the material. If material is not included in the article's Creative Commons licence and your intended use is not permitted by statutory regulation or exceeds the permitted use, you will need to obtain permission directly from the copyright holder. To view a copy of this licence, visit <http://creativecommons.org/licenses/by-nc/4.0/>.

References

1. The American Cancer Society. Cancer facts & figures 2018. Atlanta (GA): American Cancer Society; 2018.
2. Schlenk RF, Dohner K. Impact of new prognostic markers in treatment decisions in acute myeloid leukemia. *Curr Opin Hematol*. 2009;16(2):98–104.
3. Ben-Batalla I, Schultze A, Wroblewski M, Erdmann R, Heuser M, Waizenegger JS, et al. Axl, a prognostic and therapeutic target in acute myeloid leukemia mediates paracrine crosstalk of leukemia cells with bone marrow stroma. *Blood*. 2013;122(14):2443–52.
4. Park IK, Mishra A, Chandler J, Whitman SP, Marcucci G, Caligiuri MA. Inhibition of the receptor tyrosine kinase Axl impedes activation of the FLT3 internal tandem duplication in human acute myeloid leukemia: implications for Axl as a potential therapeutic target. *Blood*. 2013;121(11):2064–73.
5. Gunawardane RN, Nepomuceno RR, Rooks AM, Hunt JP, Ricono JM, Belli B, et al. Transient exposure to quizartinib mediates sustained inhibition of FLT3 signaling while specifically inducing apoptosis in FLT3-activated leukemia cells. *Mol Cancer Ther*. 2013;12(4):438–47.
6. Kampa-Schittenhelm KM, Heinrich MC, Akmut F, Dohner H, Dohner K, Schittenhelm MM. Quizartinib (AC220) is a potent second generation class III tyrosine kinase inhibitor that displays a distinct inhibition profile against mutant-FLT3, -PDGFRA and -KIT isoforms. *Mol Cancer*. 2013;12:19.
7. Cortes JE, Kantarjian H, Foran JM, Ghirdaladze D, Zodelava M, Borthakur G, et al. Phase I study of quizartinib administered daily to patients with relapsed or refractory acute myeloid leukemia irrespective of FMS-like tyrosine kinase 3-internal tandem duplication status. *J Clin Oncol*. 2013;31(29):3681–7.
8. Galanis A, Levis M. Inhibition of c-Kit by tyrosine kinase inhibitors. *Haematologica*. 2015;100(3):e77–9.
9. Nybakken GE, Canaani J, Roy D, Morrisette JD, Watt CD, Shah NP, et al. Quizartinib elicits differential responses that correlate with karyotype and genotype of the leukemic clone. *Leukemia*. 2016;30(6):1422–5.
10. Mori M, Kaneko N, Ueno Y, Yamada M, Tanaka R, Saito R, et al. Gilteritinib, a FLT3/AXL inhibitor, shows antileukemic activity in mouse models of FLT3 mutated acute myeloid leukemia. *Investig New Drugs*. 2017;35(5):556–65.
11. Lee LY, Hernandez D, Rajkhowa T, Smith SC, Raman JR, Nguyen B, et al. Pre-clinical studies of gilteritinib, a next-generation FLT3 inhibitor. *Blood*. 2017;129(2):257–60.
12. Perl AE, Altman JK, Cortes J, Smith C, Litzow M, Baer MR, et al. Selective inhibition of FLT3 by gilteritinib in relapsed/refractory acute myeloid leukemia: a multicenter, first-in-human, open-label, phase 1/2 study. *Lancet Oncol*. 2017;18(8):1061–75.
13. Niwa T, Imagawa Y, Yamazaki H. Drug interactions between nine antifungal agents and drugs metabolized by human cytochromes P450. *Curr Drug Metab*. 2014;15(7):651–79.
14. Scheife RT, Hines LE, Boyce RD, Chung SP, Momper JD, Sommer CD, et al. Consensus recommendations for systematic evaluation of drug-drug interaction evidence for clinical decision support. *Drug Saf*. 2015;38(2):197–206.
15. Faucette S, Wagh S, Trivedi A, Venkatakrishnan K, Gupta N. Reverse translation of US Food and Drug Administration reviews of oncology new molecular entities approved in 2011–2017: lessons learned for anticancer drug development. *Clin Transl Sci*. 2018;11(2):123–46.
16. Shah RR, Roberts SA, Shah DR. A fresh perspective on comparing the FDA and the CHMP/EMA: approval of antineoplastic tyrosine kinase inhibitors. *Br J Clin Pharmacol*. 2013;76(3):396–411.
17. Hartmann JT, Haap M, Kopp HG, Lipp HP. Tyrosine kinase inhibitors: a review on pharmacology, metabolism and side effects. *Curr Drug Metab*. 2009;10(5):470–81.
18. Herviou P, Thivat E, Richard D, Roche L, Dohou J, Pouget M, et al. Therapeutic drug monitoring and tyrosine kinase inhibitors. *Oncol Lett*. 2016;12(2):1223–32.
19. US FDA. Rifadin (rifampin capsules USP) and Rifadin IV (rifampin for injection USP). 2010. https://www.accessdata.fda.gov/drugsatfda_docs/label/2010/050420s073,050627s012lbl.pdf. Accessed 10 Oct 2019.
20. Kapetas AJ, Sorich MJ, Rodrigues AD, Rowland A. Guidance for rifampin and midazolam dosing protocols to study intestinal and hepatic cytochrome P450 (CYP) 3A4 induction and de-induction. *AAPS J*. 2019;21(5):78.
21. Almond LM, Mukadam S, Gardner I, Okialda K, Wong S, Hatley O, et al. Prediction of drug-drug interactions arising from CYP3A induction using a physiologically based dynamic model. *Drug Metab Dispos*. 2016;44(6):821–32.
22. Smith CC, Levis MJ, Litzow MR, Perl AE, Altman JK, Gill S, et al. Pharmacokinetics and pharmacodynamics of gilteritinib in patients with relapsed or refractory acute myeloid leukemia. *J Clin Oncol*. 2016;34(15_Suppl.):76.

Affiliations

Angela Joubert James¹ · Catherine C. Smith² · Mark Litzow³ · Alexander E. Perl⁴ · Jessica K. Altman⁵ · Dale Shepard⁶ · Takeshi Kadokura⁷ · Kinya Souda⁷ · Melanie Patton¹ · Zheng Lu¹ · Chaofeng Liu¹ · Selina Moy¹ · Mark J. Levis⁸ · Erkut Bahceci¹

¹ Astellas Pharma US, Inc., 1 Astellas Way, Northbrook, IL 60062, USA

² University of California San Francisco, San Francisco, CA, USA

³ Mayo Clinic, Rochester, NY, USA

⁴ University of Pennsylvania-Abramson Comprehensive Cancer Center, Philadelphia, PA, USA

⁵ Robert H. Lurie Comprehensive Cancer Center of Northwestern University, Chicago, IL, USA

⁶ Cleveland Clinic, Cleveland, OH, USA

⁷ Astellas Pharma, Inc., Tokyo, Japan

⁸ John Hopkins University, Baltimore, MD, USA